Renewable Energy 35 (2010) 412–422

Contents lists available at ScienceDirect

Renewable Energy

journal homepage: www.elsevier.com/locate/renene

Wind tunnel and numerical study of a small vertical axis wind turbine

Robert Howell*, Ning Qin, Jonathan Edwards, Naveed Durrani

Department of Mechanical Engineering, University of Sheffield, Sir Frederick Mappin Building, Mappin Street, Sheffield S1 3JD, UK

ARTICLE INFO

Article history:
Received 19 January 2009
Accepted 20 July 2009
Available online 1 September 2009

Keywords:
Wind turbine
VAWT
HAWT
Wind tunnel
CFD

ABSTRACT

This paper presents a combined experimental and computational study into the aerodynamics and performance of a small scale vertical axis wind turbine (VAWT). Wind tunnel tests were carried out to ascertain overall performance of the turbine and two- and three-dimensional unsteady computational fluid dynamics (CFD) models were generated to help understand the aerodynamics of this performance.

Wind tunnel performance results are presented for cases of different wind velocity, tip-speed ratio and solidity as well as rotor blade surface finish. It is shown experimentally that the surface roughness on the turbine rotor blades has a significant effect on performance. Below a critical wind speed (Reynolds number of 30,000) the performance of the turbine is degraded by a smooth rotor surface finish but above it, the turbine performance is enhanced by a smooth surface finish. Both two bladed and three bladed rotors were tested and a significant increase in performance coefficient is observed for the higher solidity rotors (three bladed rotors) over most of the operating range. Dynamic stalling behaviour and the resulting large and rapid changes in force coefficients and the rotor torque are shown to be the likely cause of changes to rotor pitch angle that occurred during early testing. This small change in pitch angle caused significant decreases in performance.

The performance coefficient predicted by the two dimensional computational model is significantly higher than that of the experimental and the three-dimensional CFD model. The predictions show that the presence of the over tip vortices in the 3D simulations is responsible for producing the large difference in efficiency compared to the 2D predictions. The dynamic behaviour of the over tip vortex as a rotor blade rotates through each revolution is also explored in the paper.

1. Introduction

As a sustainable energy resource, wind energy is increasingly important in national and international energy policy in response to climate change. Many large scale commercial wind farms have been built in the UK and electricity generation from wind now exceeds 3.6 GW and is increasing rapidly. To meet its obligations under the Kyoto Protocol the UK Government has adopted a target for renewable energy generation of 10% of UK consumption by 2010, 15% by 2015 and an aspiration of 20% by 2020 [1]. Much of this, by necessity, must be met by wind energy. In addition, the EU Commission has set a European target for 2010 of 12% of electricity generation from renewable sources.

The two primary types of wind turbine are the horizontal axis (HAWT) and vertical axis (VAWT) machines. The horizontal axis machines are highly developed and used in all current large scale wind farms. On the other hand, the majority of research on VAWT design was carried out as long ago as the late 1970s and early 1980s, notably at the USA Department of Energy Sandia National Laboratories [2–5] and in the UK by Reading University, and Sir Robert McAlpine and Sons Ltd (through their subsidy VAWT Ltd) who erected several prototypes including a 500 kW version at Carmarthen Bay [6]. When it became accepted that HAWTs were more efficient at these large scales, interest was lost in VAWT designs and HAWTs have since dominated wind turbine designs. It is therefore not surprising that very little research can be found in the last couple of decades on the VAWT, its aerodynamics and the problem of the interaction of the blade structure with the unsteady aerodynamic loads. Their technical development lags significantly behind that of HAWTs. However, it has never been shown that HAWTs are fundamentally more aerodynamically efficient than VAWTs. Indeed it has been suggested that VAWTs may be more appropriate than HAWTs at very large scale (10 MW+) due to the alternating gravitational loading on a HAWT blade becoming excessive. There are a number of substantial advantages over HAWTs, such as:

* Corresponding author. Tel.: +44 (0)114 2227725; fax: +44 (0)114 2227890.
E-mail address: r.howell@sheffield.ac.uk (R. Howell).

0960-1481/$ – see front matter © 2009 Elsevier Ltd. All rights reserved.
doi:10.1016/j.renene.2009.07.025

- The VAWT has no need to constantly yaw into the local wind direction.
- Due to the relatively lower rotational speed, VAWTs are typically quieter than HAWTs.
- The manufacturing cost for a very large VAWT could be lower than that for an equivalent HAWT due to the simpler straight constant section blades compared to the complex three-dimensional blade shape in HAWTs.
- The VAWT is also mechanically better able to withstand higher winds through changing stalling behaviour, offering a potential operational safety advantage during gust conditions.

Considerable improvements in the understanding of VAWT can be achieved through the use of CFD and experimental measurements. The aim of this paper is to illustrate some of the improved understandings of the aerodynamics of vertical axis wind turbine performance through wind tunnel testing and computational simulation of the flow field around the turbine.

One of the constraints used with the turbine developed here was that it was to be operated at realistic wind speeds. A median wind speed of 3.5 m/s at 10 m above ground was measured at the Sheffield University weather station between 1988 and 2007. Performance measurements were taken around this wind speed as well as some measurements at higher wind speeds, but it should be born in mind that these higher speeds are rather rare, particularly in the urban environment. For example just 0.3% of the wind speeds recorded at Sheffield University's weather station were above 12 m/s. The investigators were interested in real world performance, not artificial 12 m/s 'rated' wind speeds often quoted by manufacturers.

2. Experimental set-up

The wind tunnel tests were conducted at the Aerodynamics Laboratory at Sheffield University. The University low speed wind tunnel used for this study has a square test section of dimensions 1.2 m × 1.2 m. The tunnel consists of a large bell mouth screened inlet with a contraction ratio of (2.5:1) before the flow encounters another screen and an array of honeycomb flow straighteners. The tunnel has a working section of length 3.0 m.

Any obstruction placed within a wind tunnel will alter the characteristics of the flow to some degree. If this obstruction is too large then the area available to the flow is significantly reduced, and so the speed of the flow around the model will increase. If the blockage ratio is high enough then the effects of the tunnel walls may begin to interfere with the flow over the model. The literature suggests that blockage ratios below about 6–7.5% have a negligible effect on the flow. However, the difficultly in this case comes in defining the frontal area of the turbine as it spins. The area of the wind turbine when it is stationary is small, but the area it sweeps out as it spins is significant. For the most conservative value of blockage ratio, the frontal swept area of the turbine could be used and using the wind tunnel dimensions, this would result a 20 cm × 43 cm turbine (i.e. area 0.086 m^2). Clearly this would be a tiny model, and the difficulties in testing it would be numerous including the problem that the Reynolds number would be too much smaller than that of a realistic VAWT. It was therefore more practical and reasonable to assume the apparent frontal area of the turbine would lie somewhere between the small area of the components and the large area of the swept frontal area. It was decided that blockage ratios based on frontal swept area could be tolerated beyond 7.5%, so a notable amount of the frontal swept area would not actually be occupied by the turbine. Preliminary experiments with the turbine in the wind tunnel showed that there was no correlation between the rotational speed of the wind turbine and the approach velocity within the tunnel (measured five rotor blade chords upstream). Furthermore, during the testing of the Turby VAWT [7], a turbine with blockage ratio of 14% based on frontal swept area was used with a view to it having a "negligible blockage effect".

2.1. Aerofoil selection

Traditionally NACA 4-digit series have been employed for Darrieus-type VAWTs. For example, a NACA0015 profile has been used in the Sandia investigations. In the late 1970s, Healy investigated the effect of thickness on VAWT performance [8]. More recently, a systematic numerical study of various aerofoils including NACA 4-digit series based on the unsteady RANS solutions of the VAWT flows by the authors indicated that thicker sections performed much better under the flow conditions of interest. As a result of our simulations, the NACA0022 profile was chosen as the primary profile candidate for this research programme. In order to create a geometrically accurate profile the rotor blades were manufactured using CNC milling machine from high-density foam. In order to give the blades sufficient strength to withstand the centrifugal bending forces cause by the high rotational speeds of the turbine, the foam had to be of a minimum thickness. The NACA0022 profile was therefore created with a thickness of 22 mm and a resulting chord of 100 mm. This, combined with a height of 400 mm (limited by the CNC machine), gave the blades an aspect ratio of 4 and gave the turbine a solidity of 1.0 for the three bladed turbine and a value of 0.67 for the two bladed turbine. These values are rather high given other research clearly shows a lower solidity will result in a higher performance coefficient. However, the aim of this research turbine was to provide validation data for computational methods and an understanding of the aerodynamic inefficiency (such as those generated by the tip flows and resulting vorticies) so maximum performance in itself was unimportant. As will be shown later, the low aspect ratio did indeed give rise to large tip vorticies. Testing was carried out using 300 mm rotor arms resulting in a blockage ratio (based on frontal swept area) 16.7%.

During initial testing at some conditions, the turbine would suddenly reduce its rotation speed and eventually stop despite no changes to the applied torque. It transpired that the turbine blades were slowly rotating about an axis centred through the bolts that fix them to the support struts. This was caused by the centre of rotor lift not being aligned properly with the fixing bolts. It is clear that the centre of lift for VAWT rotor blades is constantly changing throughout every rotation so it was not a simple process to determine the best location of the fixing holes on the rotors. The maximum change in the rotor blade fixing angle was measured to be less than 5° and this small angle change caused a complete loss of lift and hence the eventual complete loss of power from the turbine.

A CAD model was used to carry out the design before manufacture, see Fig. 1. Two deep-grove ball race bearings were used to support the turbine and allow free rotation of the rotor shaft, where the lower bearing supporting the weight of the turbine by acting as thrust bearings. Two support arm/strut brackets were designed to fit on the main drive shaft so that they could be mounted anywhere along the height of the shaft accommodating 2, 3 or 4 blades to accommodate future blades of different lengths (aspect ratios). Rotor blade radial arms/spokes were machined from aluminium bars and aerodynamically profiled with an elliptical leading edge (major to minor axis ratio of 2:1) and sharp trailing edge. All components were attached such that they could be assembled or adjusted with ease. The finished assembly is pictured in Fig. 1.

To measure the power output from the turbine a simple torque brake was employed. The torque applied to the turbine rotor drive

Fig. 1. CAD model of the turbine model assembly and the model turbine in the wind tunnel.

shaft was increased and decreased by changing the separation distance between two spring balances. The torque applied was calculated using the difference in the forces applied by the spring balances and the drive shaft radius. To calculate the power output, this torque was combined with the rotational speed of the turbine, itself picked up from a once per revolution optical tachometer. A feedback control system was not used for the control of the turbine so it was not possible to measure the characteristics of the turbine past its maximum torque (and therefore minimum stable rotational speed). This is because beyond this limit any small increase in applied load (torque) causes a drop in the rotation speed of the turbine and a drop in the lift (and driving torque) it generates. If there is no control system to reduce the applied torque to match the new aerodynamics condition, the turbine rotor will continue to drop in speed so the applied torque becomes more unmatched to the conditions of the slower rotating turbine.

3. Experimental results

This section presents the results obtained from the wind turbine measurement campaign; however the effect of bearing and windage losses must first be explained. To determine the amount of power lost in the system a series of spin down tests were conducted. To increase the moment of inertia of the system once the foam rotor blades had been removed, small weights were attached to the ends of the support spokes. The rotor system was manually spun up to slightly beyond the maximum speed used in the turbine performance testing and then allowed to freely decrease in velocity due to the effects of friction in the bearings and windage on the support arms and the added weights. As the speed reduced, the time and instantaneous rotor rpm were recorded. From this information, it was possible to calculate the bearing and windage losses of the system (with its known moment of inertia) without the rotor blades attached. In this paper, the power used to overcome these losses is actually included in the stated power output from the turbine. Clearly this is not useful power output, but it is still the power developed by the turbine in overcoming losses as well as generating useful work in the torque brake and is the correct value to be compared to the CFD results. In a turbine of this size the bearing losses are significant and so must therefore be carefully analysed.

Fig. 2 shows how the measured torque due to bearing friction and windage changed with tip-speed ratio as well as the torque applied by the brake for the same conditions. It is clear that at high

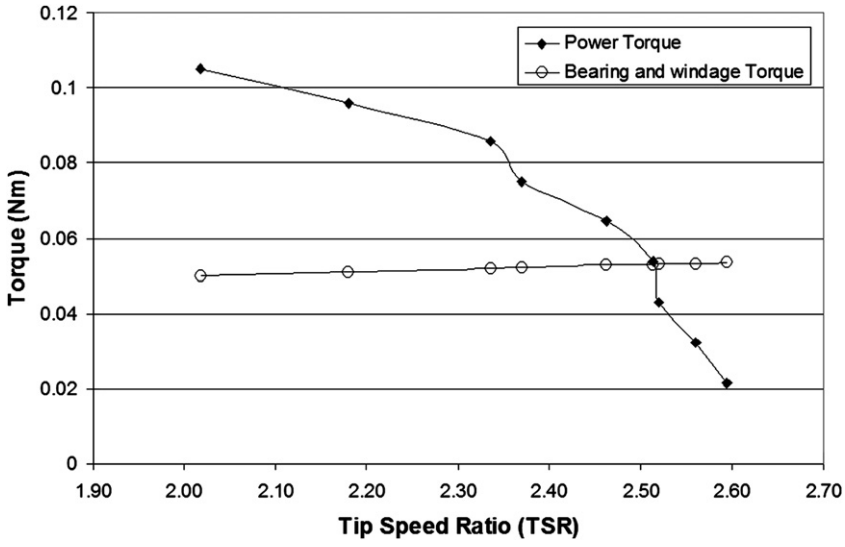

Fig. 2. Measured bearing and windage torque versus power torque developed by the turbine for a wind speed of 5.07 m/s.

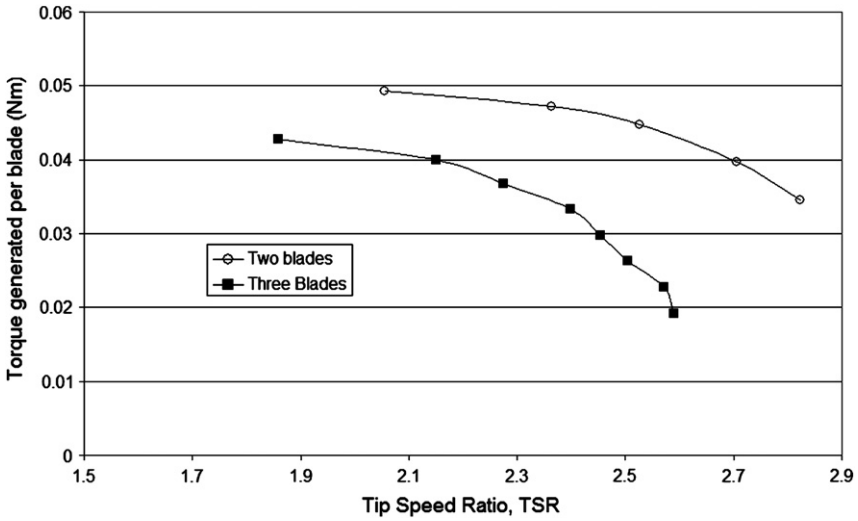

Fig. 3. Variation of torque per blade with rotational velocity at 5.07 m/s wind velocity for 2 and 3 blade turbines.

tip-speed ratios, the torque caused by the losses generated in the bearings, support arms and windage in the system are double that of the applied braking torque. This means any error in the measurement of the windage torque will have a very significant effect on the performance coefficient. At the other end of the performance envelope, at a tip-speed ratio of around 2, the applied braking torque is more than double the windage torque, but none the less this torque 'loss' is still very significant.

The power losses due to bearing friction and windage are a complex function of tip-speed ratio. This is due to the changing nature of the physics involved in the bearing dynamics and the aerodynamics. At low values of TSR the flow over (parts of) the support arms and the added masses will be laminar and result one value of drag coefficient, whereas at higher values of TSR the flow is likely to be turbulent. The losses in the bearings will also alter due to changes in the oil film thickness which is itself a function of rotational speed as well as other bearing parameters. It should also be noted that given the large percentage of the total power lost in the bearings (and windage), the turbine was left rotating for at least 30 min to warm up before any performance measurements were taken.

From the measurements of the rate at which the rotor slowed its rotation speed at different wind speeds, the losses due to windage and bearing friction were calculated and curve-fits generated. During the performance mapping studies, the wind turbine performance was measured using the torque brake and then a curve fit polynomial was then used (as appropriate for each wind speed) to calculate windage and bearing power losses that the turbine was overcoming. The brake measurements and the losses were then added to give the total power developed by the turbine.

A sensitivity analysis was carried out, whereby the drag coefficient of the added weights was altered and the resulting changes on the overall performance coefficient were noted. In addition, an error analysis was conducted by accounting for the accuracy of the once per revolution trigger (used to obtain the rotational speed) and also the accuracy of the spring balances used. The accuracy of these results is overwhelming determined by the accuracy with which the losses due to windage and bearing friction. The added weights used to increase the moment of inertia of the rotor assembly where of approximately cylindrical shape, and so a drag coefficient appropriate to this shape and the Reynolds number

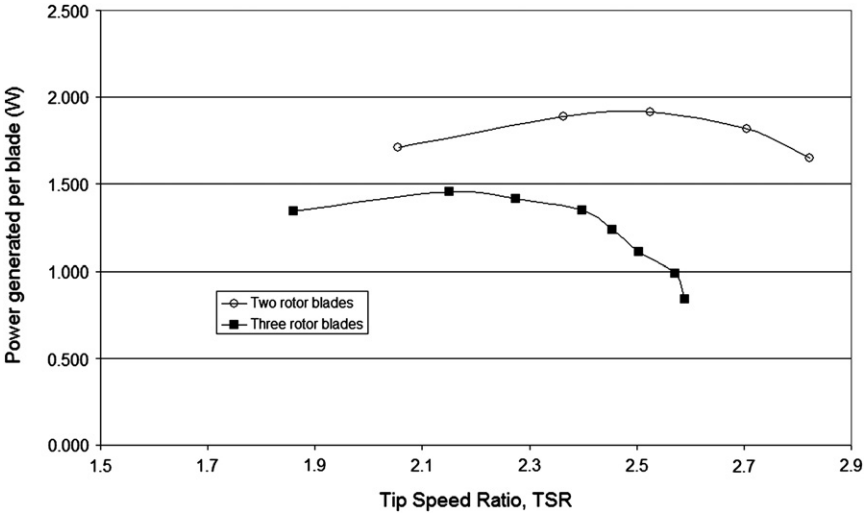

Fig. 4. Variation of power per blade with rotational velocity at 5.07 m/s wind velocity, for 2 and 3 blade turbines. Surface finish on blades: smooth.

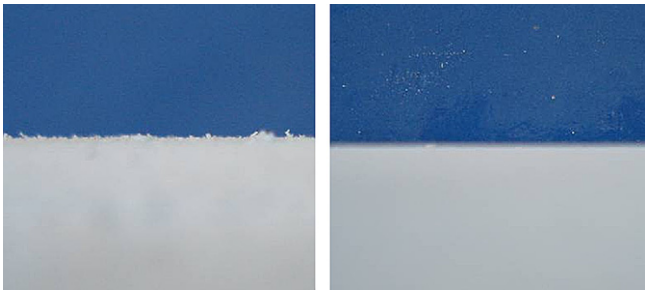

Fig. 5. Blade surface roughness before and after surface smoothing treatment.

encountered was used. However, this Reynolds number changed as the rotor assembly slowed its rotation speed and so there is another complication in determining the appropriate drag coefficient to use. The shape of the weights was also only approximately that of a cylinder which also complicates matters. Overall, this significantly complicates the analysis of the errors.

The maximum overall error in the determination of the power developed by the turbine is approximately 20%. Despite this absolute error, repeatability is extremely good. For a number of wind speeds the turbine was repeated moved through its range of TSR by changing the applied torque and the repeatability was within 5%. It will therefore be possible to compare changes in operating condition of the CFD and experimental model within 5% but we can expect to see differences in absolute power coefficients between simulation and experiment of 20%.

3.1. Effects of solidity on performance

Solidity is one of the main parameters dictating the rotational velocity at which the turbine reaches its maximum performance coefficient. Higher solidity usually dictates lower tip-speed ratio and lower efficiency. At low tip-speed ratios, the rotor blades do not interact as strongly with much of the air flow passing through the volume swept out by the proceeding blades, but at high tip-speed ratios, rotor blades begin to interact with the wakes strongly from upstream blades.

As has been noted already, the solidity of this rotor blade was rather high (for structural reasons) so the tip-speed ratios (TSRs) seen in Fig. 3 are on the low side compared to other turbines. Kirke (1998) [11] collected together data from other turbine tests with a variety of tip-speed ratios and illustrated that maximum efficiency for those turbines was attained with a TSR of 3 and 5. At lower TSRs (between 2 and 3) that data showed maximum performance coefficients of less than 30%. Given the aspect ratio of this turbine it is expected that the performance coefficients will be lower still and was actually expected to be around 20%.

The effect of solidity is shown for the two and three blade turbine models in Fig. 3, both models display a similar value of maximum torque but the two blade turbine's maxima lie at a low value of tip-speed ratio because of the lower solidity of the design. This will be due to the ratio of the lift to drag on the two bladed turbine being proportionally higher than the three bladed design and thus generating higher torque and higher rotational speeds for a given TSR. As rotational speed increases, the torque on the two blade machine decreases at a lower rate to that of the three blade machine. Although the maximum torque per blade was very close for the two and three bladed turbine models, the power per blade was higher for the two blade turbine model, as it developed the maximum torque at a higher rotational velocity, see Fig. 4.

Fig. 4 also shows that adding more blades (with the same chord) has a reduced benefit; as the blade number increases each blade added adds another wake and lowers the rotational velocity at which optimum performance is achieved. Literature relating to HAWTs shows similar conclusions. High solidity machines are traditionally used for high torque, low speed operation, such as water pumping; low solidity machines are used for low torque, high speed operations, such as electrical power production. The benefit of adding more blades depends on a trade off between the various required performance characteristics and manufacturing costs. Other parameters that may be affected by the number of blades include, rotor weight and balance, structural loading, torque ripple, starting torque, and fatigue resistance. It should be noted here that the number of blades was increased, but the chord of those blades was not reduced so the solidity rises substantially.

3.2. The effect of surface roughness

With the correct level of surface roughness, it is possible to trip a boundary layer from laminar to turbulent flow at a lower Reynolds number than for a flow on a smooth surface and this usually

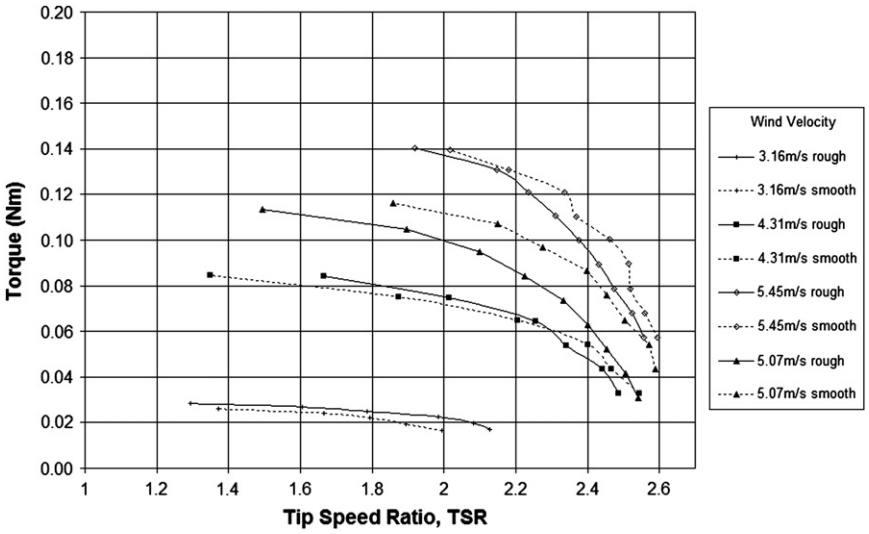

Fig. 6. Torque variation with rotational velocity for turbine model with three blades, for smooth and rough blade surfaces.

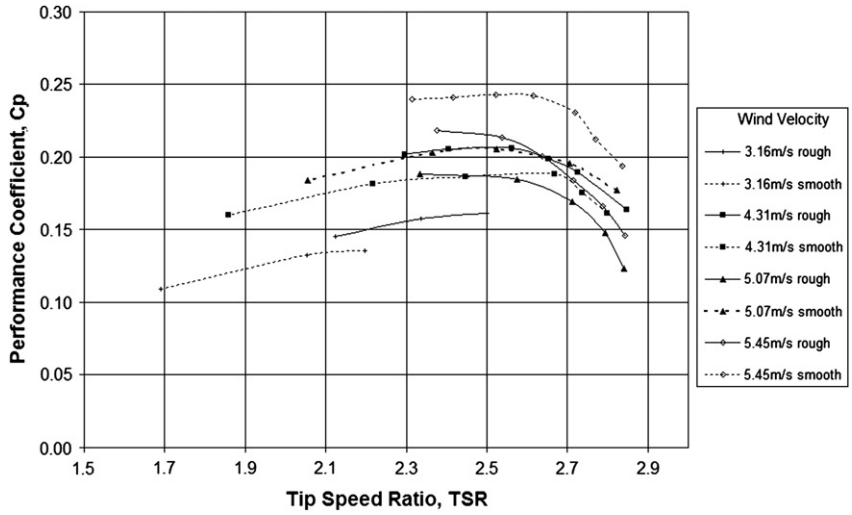

Fig. 7. C_P variation with rotational velocity for turbine model with two blades, for smooth and rough blade surfaces.

causes an increase in drag. However, a turbulent boundary layer will also be more resistant to flow separation from the rotor blade surface and so it is possible for the drag to be reduced with turbulent flow where a separation was present with laminar flow, i.e. although skin drag has increased form drag and therefore overall drag on the aerofoil is reduced.

The surface finish on the blades due to the manufacturing process was visibly rough. Unfortunately since blades were manufactured from high-density foam, it was not possible to use a surface profiler to determine the exact size of surface roughness. However, using a roughness feeler gauge it was estimated that the largest scales of roughness were approximately 0.5 mm in height, giving a non-dimensional roughness of (x/C) equal to 0.005. The turbine rotor blades were initially tested with the blades in this as-manufactured state. The model was then tested after the blades had been smoothed by hand using fine-grade glass paper after which the normalised roughness was estimated (again using the roughness feeler gauge) to be approximately 0.0005, i.e. an order of magnitude lower than in the previous case. It should be noted that any change in profile *shape* was negligible after sanding with the glass paper. Fig. 5 shows qualitatively that the difference in surface roughness before and after treatment was significant.

From Fig. 6, it can be clearly seen that the surface roughness had a significant effect on the performance coefficient of the model turbine. At lower wind velocities (below a Reynolds number of 30,000, i.e. a wind speed of 4.3 m/s), smoothing the surface of the blades reduced performance quite significantly in both the two and three blade test cases. It is hypothesised that is due to the rougher surface undergoing a laminar to turbulent boundary layer transition much earlier, and so being more inclined to stay attached to the aerofoil surface and so resulting in a lower drag on the aerofoil.

It is interesting to note that for a wind speed of 4.31 m/s, the performance curves for smooth and rough blades cross at a tip-speed ratio of just over 2.2. The traditional definition of Reynolds number for a wind turbine remains constant for a constant wind speed, but there appears to be a dependency in this data if we consider the Reynolds number *that the flow sees* is dependent on the rotor relative wind speed. This is not surprising. The Reynolds number over a VAWT rotor blade changes continually as it rotates both towards the oncoming wind and against it, i.e. windward and

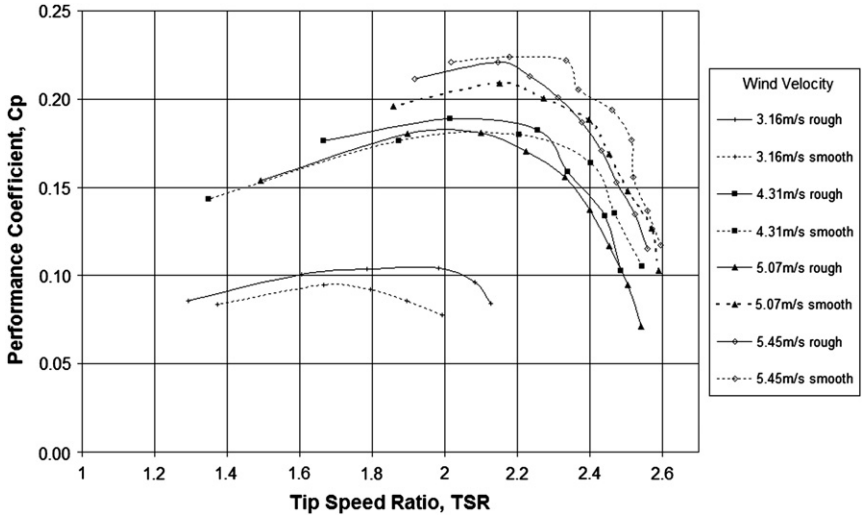

Fig. 8. C_P variation with rotational velocity for turbine model with three blades, for smooth and rough blade surfaces.

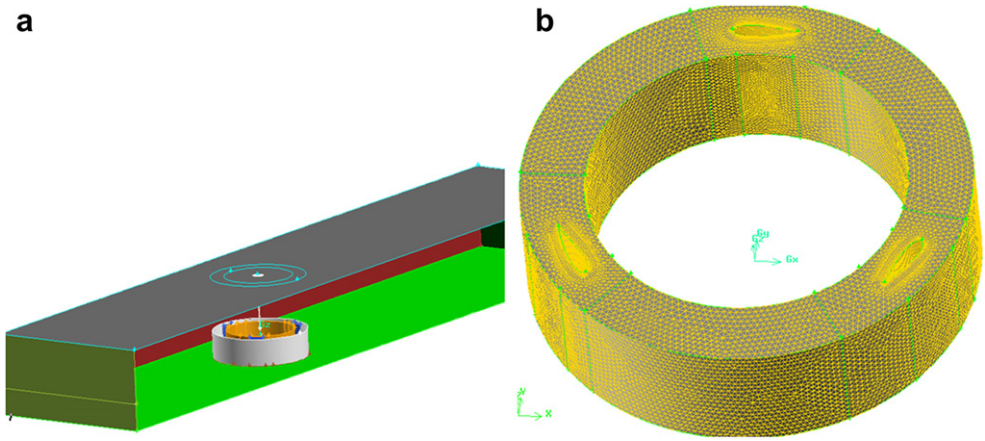

Fig. 9. Computational domain (a) for the three-dimensional simulations and details of the moving mesh (b) used to model the rotor blades.

leeward. As the rotational speed of the turbine increases (at low applied torques, for example), the maximum relative velocity increases and so does the maximum Reynolds number. It is of course possible with the correct tip-speed ratio for the minimum leeward Reynolds number to drop to zero. With these Reynolds number changes occurring, it is therefore not surprising that such a cross over in the performance curves occurs.

Above a critical Reynolds number the above figures shows that in both two and three blade tests, the maximum torque obtained for blades with rough surfaces was obtained at a lower tip-speed ratios than for smooth blades. At a lower tip-speed ratios, there exists a larger variation in the angle of attack than at higher TSRs. From Fig. 6 it seems that a blade with a rough leading edge is likely to help delay the onset of stall which is more likely to occur at the high angles of attack. It should be noted that the maximum torque point was difficult to measure being a rather unstable operating point with the torque brake used there.

Adding boundary layer trips may have improved performance at low Reynolds numbers without reducing performance at higher velocities by causing an increase in skin friction drag, or compromising the leading edge. Researchers at Sandia Laboratories [5] found flaking paint on the leading edge resulted in a boundary layer trip that reduced efficiency, as the blades were natural laminar flow blades designed to maintain a laminar boundary layer for a long proportion of their chord length. It is likely that as this roughness directly on the leading edge may have also delayed separation into stall.

As can be seen from Figs. 7 and 8 the maximum performance coefficient of this turbine is around 25% and occurs at the maximum wind speed and therefore the maximum Reynolds number tested. At the maximum TSR (around 2.8 for the two blade and around 2.5 for the three blade design), the angle of attack variation seen by each the rotor blades at each wind speed will be the identical. Therefore the only difference (apart from surface finish) between the cases, is the Reynolds number and it is clear this has a significant effect on the performance on the two bladed (low solidity design) but a smaller effect on the three blade design.

4. Numerical simulation and comparison to experimental measurements

This section provides a comparison between the experimental measurements and the computational predictions carried out to more fully understand the flow structures around the model turbine. The computational fluid dynamics code used was Fluent while the mesh generation was carried out using Gambit. Having achieved mesh independence and suitable $Y+$ values of less than 10 (and using wall functions, but not enhanced wall functions) this

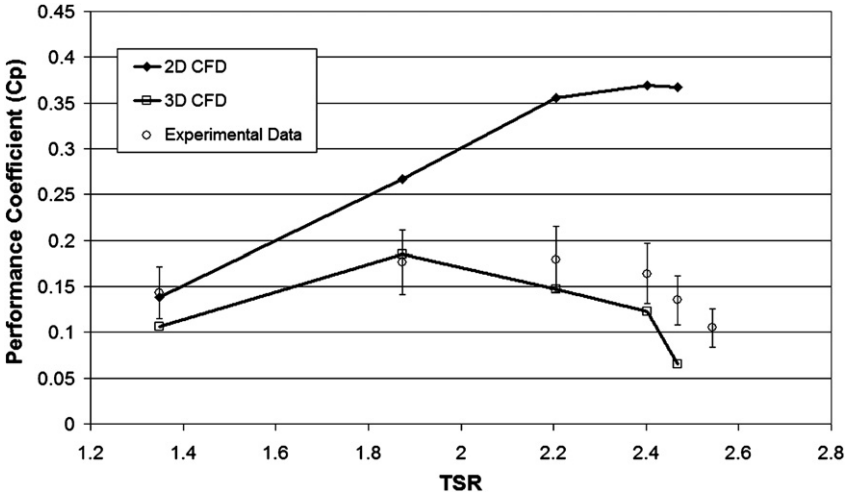

Fig. 10. Performance coefficient for the model turbine and the simulations at a wind speed of 4.31 m/s.

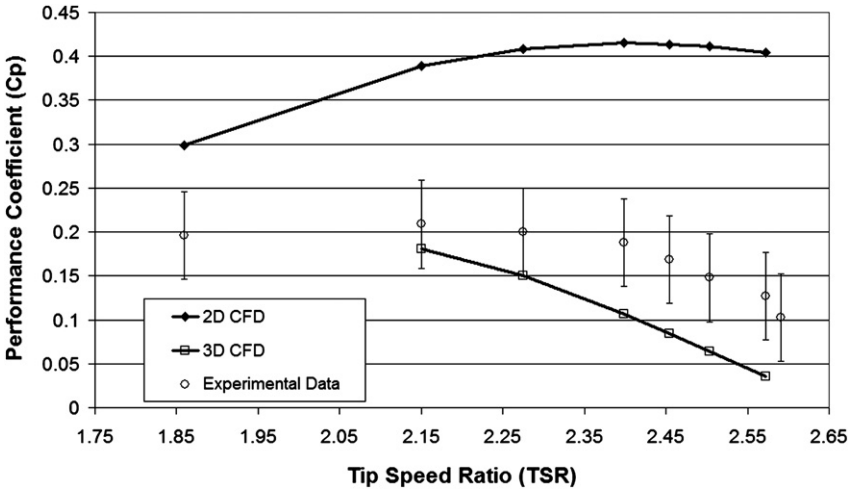

Fig. 11. Performance coefficient for the model turbine and for the simulations at a wind speed of 5.07 m/s.

resulted in a 3D model with approximately 1.3 million cells, as shown in Fig. 9. The solutions were initially obtained using first-order discretisation until periodic solutions were achieved (usually after approximately 3 or four rotor revolutions) and after this the spatial discritisation was switched to the more accurate second order spatial discretisation.

The choice of the turbulence models influences the resultant flow field and the computational resource and time required to achieve solutions. For HAWTs it was found that standard k–ϵ model gave inaccurate results after flow separation in the previous research done by Wolfe and Ochs [9]. However, the k–ϵ RNG model is known to predict flow fields involving large flow separations more accurately so for the present task, k–ϵ RNG turbulence model was used.

The entire flow domain is shown in Fig. 9a, which models the wind turbine and accurately models the side walls and roof of the wind tunnel relative to the turbine. The wind tunnel walls were included in the model as it is expected that the effects of the wind tunnel wall could be significant, considering the relative size of the model rotor to that of the test section. The front of the domain was defined with boundary condition Velocity Inlet, which allowed the magnitude of inlet flow and turbulent quantities to be specified. The turbulent intensity of 1% and length scale of 0.01 m were applied to approximately account for the incoming flow turbulence in the wind tunnel. The outlet of the domain was defined with the boundary condition Outflow. The top, bottom and sides of the domain are defined as non slip walls. It should be noted that the inlet and output boundaries are not placed in representative positions relatively to the wind turbine in the wind tunnel, but are instead further away. This avoids the potential problem of computational boundaries interacting with the flow around the turbine. A sliding mesh geometry was used to model the rotor geometry and can be seen in Fig. 9b and a symmetry plane was used at rotor mid span to ease the computational requirements.

4.1. Predicted turbine performance

Fig. 10 shows the effect of changes in turbine operating point on the coefficient of performance for both the experimental measurement, two dimensional and full three-dimensional CFD at a wind speed of 4.31 m/s. The error bars on all the experimental data is fixed at a value of ±20% of the measured value. There is reasonable agreement in both the level and the shape of the 3D predictions and the experimental measurements, which gives confidence that the 3D CFD is correctly capturing the essential flow physics of the aerodynamics. It should be noted that at this Reynolds number of 30,000, the agreement between the 3D predictions and the experimental data tends to diverge towards higher

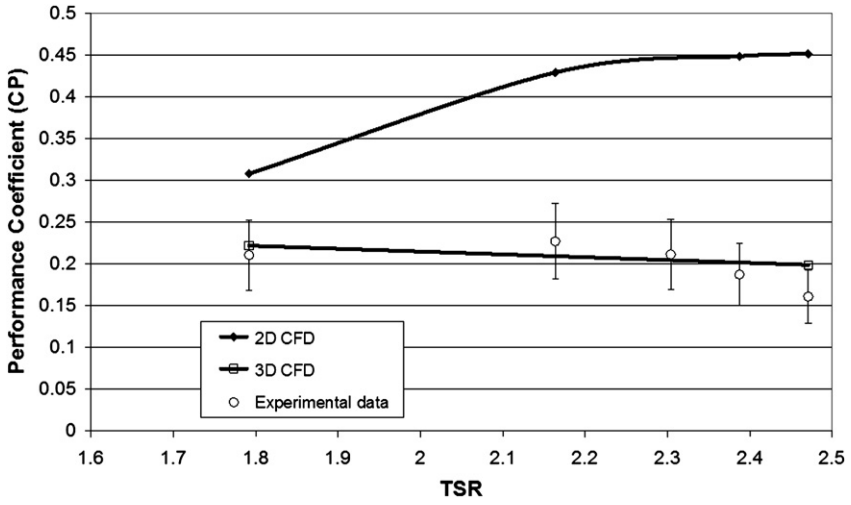

Fig. 12. Performance coefficient for the model turbine and simulations for a wind speed of 5.81 m/s.

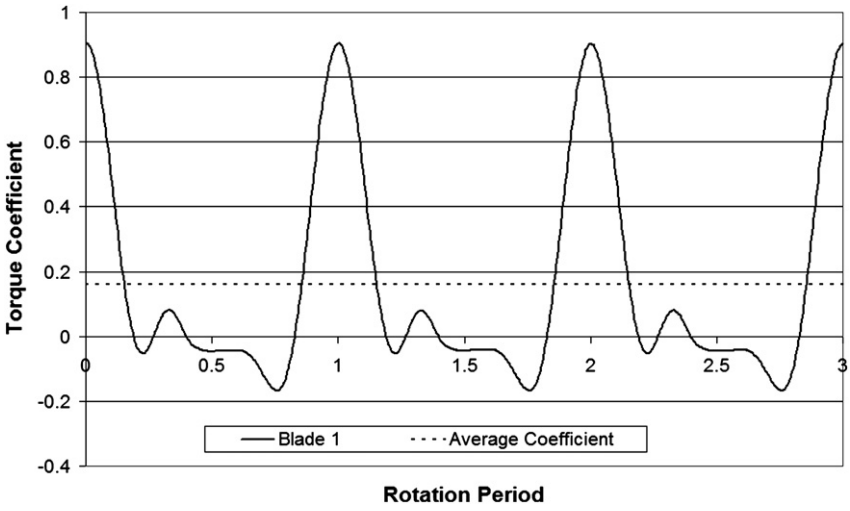

Fig. 13. Predicted torque coefficient for a single rotor blade from 2D simulations.

tip-speed ratios. Fig. 11 shows the results for simulations and experiments carried out at a wind speed of 5.07 m/s or a Reynolds number of around 34,000. Once again the 3D simulations are underpredicting the performance coefficient, particularly at the higher tip-speed ratios. At higher tips speed ratios, the changes in angle of attack between the relative velocity vector and the rotor blades reduce. As such one might expect the agreement between simulation and experiment to improve at higher tip-speed ratios, but this is clearly not the case here. The 3D simulations do not include the radial support arms, so if these were included there would be an additional drag force on the turbine and as a result an even lower power performance coefficient. This would make the simulated results move even further way from the experimental data.

Fig. 12 shows the performance coefficient for a wind speed of 5.81 m/s or a Reynolds number of 39,000. Although results at only two tip-speed ratios are presented for the simulations, it seems that the results are now closer than at lower Reynolds numbers. The peak in performance coefficient does not seem to change at all in the experimental data as the Reynolds number has increased as it remains at around a tip-speed ratio of 2.1 to 2.2. As seen in earlier figures of experimental data alone, the performance coefficient generally increases with Reynolds number. This is also the case for the 2D and the 3D simulations over most of the range of tip-speed ratios. This increase in performance is likely to be due to the changing stall behaviour as separation bubbles transition from an initial laminar shear layer earlier along the blade surface than at lower Reynolds numbers.

The overall difference between the predicted 2D performance and the experimental and 3D CFD results is believed to be caused by a number of reasons. The main one will be that, of course, the 2D CFD simulation does not include the effects of the tip vortices present on the real turbine and the 3D simulations. A simple analysis of the drag losses caused by the support spokes showed that these aerodynamic losses were rather small. This analysis was carried out by calculating the drag losses on an elemental section of the support spoke using an appropriate drag coefficient and the local relatively velocity. These losses were integrated from root to the tip of the support spoke give the total loss. The overwhelming reason therefore for the difference between the 2D and the experimental results and the 3D CFD simulation is caused by the rotor tip vortices present on each end of each rotor blade. It should be noted that the 3D CFD geometry does include the central drive shaft, but does not include the support spokes so one would expect to see a difference between those results and the measurements, quite apart from the experimental and numerical accuracy.

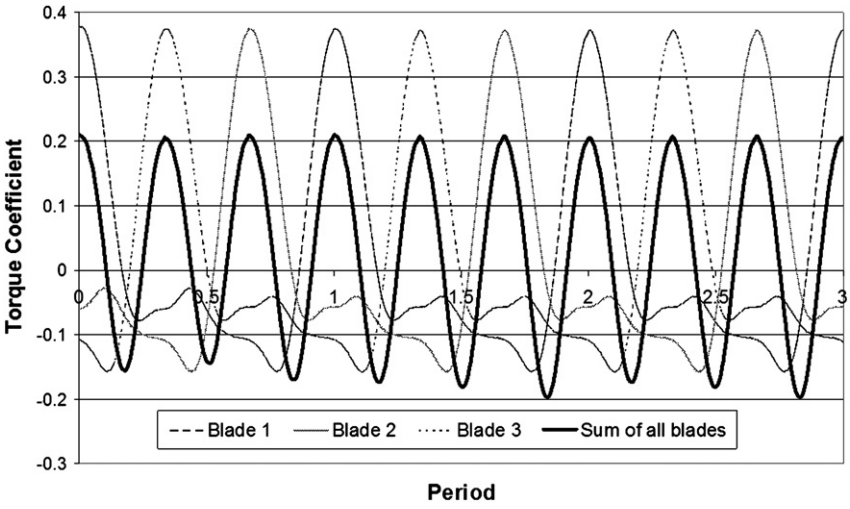

Fig. 14. Predicted torque coefficient for three individual rotor blades and the total torque developed by the turbine as predicted by 3D simulation.

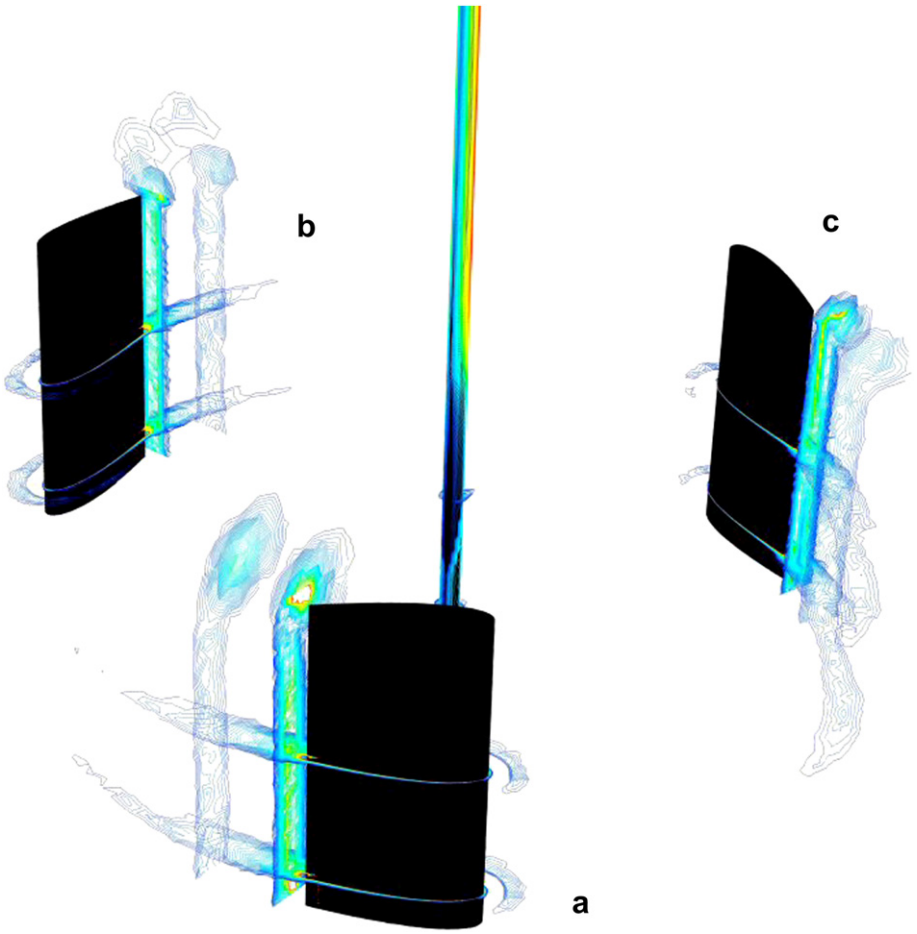

Fig. 15. Contours of vorticity for the three rotor blades illustrating the changing strength of the tip vortex for the rotors at different phases. 415 rpm, $V_\infty = 5.07$ m/s.

The predicted torque output of a single rotor blade as predicted by the 2D simulations is shown in Fig. 13. The torque curve is characterised by a high and fairly narrow peak in torque coefficient. There is very little negative torque developed as the rotor blades travel through the stall regions (time periods of between 0.25 and 0.8). The details of the stall development and its relationship to the torque ripple in a similar turbine is discussed in [10].

The torque output from the equivalent 3D simulations is shown in Fig. 14. Overall the shape of the torque peaks is similar to those in Fig. 13, but the shape of the torque curve between the peaks has change character indicating different flow physics are at work and most importantly, the overall torque level has dropped considerably. The reason for this must be due to the presence of the tip vortices.

4.2. Detailed turbine aerodynamics

In an effort to determine some of the more important flow physics occurring during the full 3D simulations, plans were used to visualise the vorticity shed from the rotor blades. The planes were set up at distances of 10% and 50% downstream of the rotor trailing edges and also at just above mid span and 75% span as shown in Fig. 15.

The wind velocity vector in this direction is into the page. From the vertical visualisation plans, it is possible to see the variation in the strength of the over tip vortex as the rotor blades find themselves at different phase angles. Shortly after the rotor blade develops maximum lift (not necessarily the same as maximum torque in Fig. 14) the tip vortex will be at maximum strength and this appears to be the case for rotor blade (a). The intensity of the vortex core and its extent are at a maximum for this rotor blade and at this location (phase). As this rotor blade reaches the location of rotor (c) the extent of the over tip vorticity has reduced, while by the time the rotor reaches the location of blade (b), it appears to be at a minimum.

This changing in strength is due to the changing lift developed by the turbine rotor blade as it rotates through different phase angles. It should be noted that there is likely to be a small delay between maximum lift being developed and the maximum strength of the tip vortex occurring. This will simply be due to the time required for the flow to respond to the changing lift around the rotor blade.

A horizontal visualisation plan has been used at the tip of the rotor blades in Fig. 16 to further illustrate the strength of the vorticity of the over tip flow. It is very clear from this figure that the wake caused by the tip vortex extends to a considerable proportion of the area swept out by the rotor blade. The region marked 'W' in Fig. 16 is the wake from the previous rotor and at the instant shown in this figure is about to flow past the central support strut. As the wake segment continues to flow downstream, it will actually interact with the rotor that created it. This will cause changes in both the surface pressure distribution of that rotor blade, but may also change the laminar to turbulent flow transition locations in the rotor blade. This is due to the elevated levels of turbulence in the

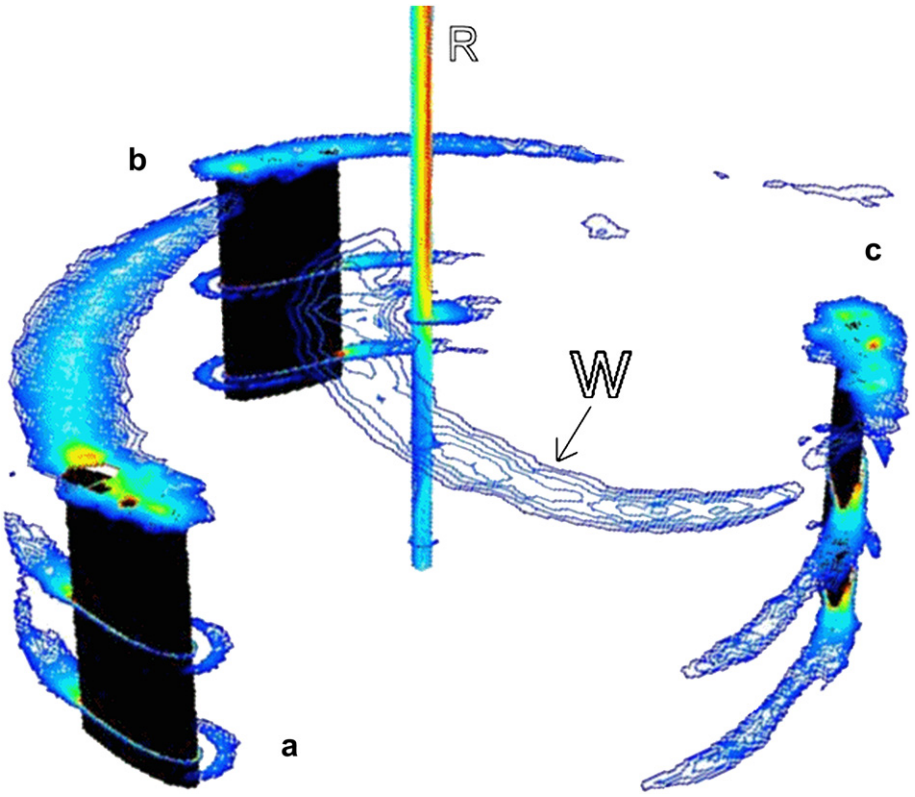

Fig. 16. Contours of vorticity for the three rotor blades illustrating the changing strength of the tip vortex for the rotors at different phases. 415 rpm, $V_\infty = 5.07$ m/s.

wake and the relatively low Reynolds numbers of the flow over this rotor. It should be noted that such flow physics are not captured in these simulations, but are potentially present in the wind tunnel model.

5. Conclusions

A small model research VAWT turbine has been manufactured and tested over a range of operating conditions. The straight turbine rotor blade, with an aspect ratio of 4:1, operates at relatively low tip speeds and its performance shows a clear dependence on the rotor blade surface finish. Below a critical Reynolds number (30,000), the performance is enhanced by having the surface of the turbine roughened, but above this Reynolds number the power coefficient is degraded. The tests also shows that the two and three bladed rotor models produces similar peaks in performance coefficient, but that the three bladed design did so at a much reduced TSR.

Computational predictions of the performance coefficient of this turbine were carried out and the 3D simulations were shown to be in reasonably good agreement with the experimental measurements, considering errors and uncertainties in both the CFD simulations and the wind tunnel measurements. The 2D simulations showed a significantly increased performance compared to the 3D simulations and this was shown to be mainly due to the presence of the large tip vortices present in the real turbine and the 3D simulations. Simulations illustrated the periodic pulsing nature of the tip vortices caused by the changing lift generated by the rotor blades as they travel through each rotor revolution. At phases where higher amounts of lift are generated, stronger tip vortices are present, whereas at phases where little lift is generated, the vortices are significantly reduced.

References

[1] UK energy in brief. DTI Publication. URN 06/220. [accessed online 02.03.07], http://www.dti.gov.uk; July 2006.
[2] The history of the DoE program. U.S. Department of Energy, Sandia National Laboratories, American Wind Energy Association.
[3] Dodd HM. Performance predictions for an intermediate-sized VAWT based on performance of the 34-m VAWT test bed. In: Berg DE, editor. Proceedings of the ninth ASME wind energy symposium. Sandia National Laboratories; January 1990.
[4] Dodd HH, Ashwell TD, Berg DE, Ralph ME, Stephenson WA, Veers PS. Test results and status of the DOE/Sandia 34-M VAWT test bed. In: Proceedings of the Canadian wind energy association conference. Sandia National Laboratories; September 1989.
[5] Berg DE, Klimas PC, Stephenson WA. Aerodynamic design and initial performance measurements for the Sandia 34-m vertical axis wind turbine. In: Proceedings of the ninth ASME wind energy symposium. Sandia National Laboratories; January 1990. SED-VOL 9, ASME.
[6] Price TJ. UK large-scale wind power programme from 1970 to 1990: the Carmarthen Bay experiments and the musgrove vertical-axis turbines. Wind Engineering May 2006;30(3):225–42.
[7] van Bussel GJW. The development of Turby®, a small VAWT for the built environment, TU Delft, Wind Energy Section, Global wind energy conference; 2004.
[8] Healy JV. The influence of blade thickness on the output of vertical axis wind turbines. Wind Engineering 1978;2(1):1–9.
[9] Wolfe EP, Ochs SS. CFD calculations of S809 aerodynamic characteristics. AIAA aerospace sciences meeting; 1997.
[10] Hamada K, Smith TC, Durrani N, Qin N, Howell RJ. Unsteady flow simulation and dynamic stall around vertical axis wind turbine blades. AIAA aerodynamics conference Reno; 2008.
[11] Kirke BK, Evaluation of self-starting vertical axis wind turbines for stand-alone applications. PhD Thesis, Griffith University, Faculty of Engineering and Information Technology, School of Engineering, Australia, 1998. [accessed online 15.11.06], http://ariic.library.unsw.edu.au/griffith/adt-QGU20051006-001800/].